Note on global distribution of renewable energy sources

Solomon Hsiang*

Last modified: May 20, 2008

The problem of supplying energy from renewable sources looks significantly different when a global perspective is adopted. Below are figures constructed with publicly available data. Note that for all the figures using Hammer Projections, the projection is equal-area, so that energy densities[1] (depicted by colors) times the area covered is proportional to the total energy available. Some notes:

Solar. Figure (1) plots radiation at the top of the atmosphere based on geometric considerations alone [Hartman, 1994, Spencer, 1971]. Figure (2) plots a climatology for percent cloud cover in January, similar data exists for all months [Mitchell and Jones, 2005]. Combining these data by month, assuming that all clouds possess an albedo of 0.85 (this is overly conservative number that will produced an under estimate of insolation), and averaging over the year, Figure (3) illustrates the distribution of insolation available for capture at the surface. The observed structure represents the interactions of several nonlinear relationships. Regions where solar capture looks most promising include Northern Africa, Southern Africa, the Middle East, The Horn of Africa, Southern Asia and Australia.

Wind. Figure (4) plots annual average near-surface wind velocities [Trenberth et al., 1989]. Figure (5) demonstrates the seasonality of this flow, plotting average monthly velocities. The strong Northern ocean winds rely on winter-time storm tracks, while the strong Southern Ocean winds appear to be seasonally steady. Continental wind fields are significantly weaker, however central North America, Northern Africa, North and Eastern Europe and Western Australia all look somewhat promising.

Ocean currents. Figure (6) plots average current velocities near the ocean's surface (5m depth) [Carton and Giese, 2007]. Recent work on low-head hy-

*Columbia University Graduate School of Arts and Sciences, Ph.D. Program in Sustainable Development, Email: `smh2137@columbia.edu`; Web: `www.columbia.edu/~smh2137`.

[1]Velocities, rather than energies, are actually depicted. However the purpose of these plots is to demonstrate the gross features of the global distribution, which are retained under such a monotone transformation.

draulic turbines indicates that this energy may be feasibly extractable [Gorlov, 1998]. Most of the eastern coasts of continents are near to strong "western boundary currents" (along the western boundary of the *ocean*) where water flows quickly toward the pole. These flows close a larger circulation pattern of wind-driven surface waters flowing towards the equator [Pedlosky, 1998]. Eastern North America, the Caribbean, Northern South America, the East coast of Africa, Indonesia, Australia and East Asia are all near to strong western boundary currents. The equatorial Pacific and Southern oceans also posses strong, albeit remote, near-surface currents.

Geothermal. Figure (7) displays the geothermal heat flux observed at points around the globe [International Heat Flow Commission, 2008]. Note that total energy flow ($flux \times area$) cannot be be determined by these plots. Western North America, Eurasia, Indonesia, New Zealand and Eastern Africa appear to have significant sources of geothermal energy flows. Figure (8) includes all marine observations as well as continental observations. Several sources along the coast of Asia and in the center of oceans have large fluxes, although it is not clear how accessible these sources of energy are.

References

[Carton and Giese, 2007] Carton and Giese (2007). A reanalysis of ocean climate using SODA. *Monthly Weather Review*.

[Gorlov, 1998] Gorlov, A. M. (1998). Helical turbines for the gulf stream: Conceptual approach to design of a large-scale floating power farm. *Marine Technology*, 35.

[Hartman, 1994] Hartman, D. L. (1994). *Global Physical Climatology*. Academic Press.

[International Heat Flow Commission, 2008] International Heat Flow Commission, T. (last updated 2008). The global heat flow database. *Maintained by the University of North Dakota at http://www.heatflow.und.edu/data.html*.

[Mitchell and Jones, 2005] Mitchell, T. D. and Jones, P. D. (2005). An improved method of constructing a database of monthly climate observations and associated high-resolution grids. *International Journal of Climate*, 25.

[Pedlosky, 1998] Pedlosky, J. (1998). *Ocean Circulation Theory*. Springer.

[Spencer, 1971] Spencer, J. W. (1971). Fourier series representation of the positition of the sun. *Search*, 2.

[Trenberth et al., 1989] Trenberth, K., Olson, J., and Large, W. (1989). A global ocean wind stress climatology based on ECMWF analysis. *Tech. Rep. NCAR/TN-338+STR, National Center for Atmospheric Research*.

figures

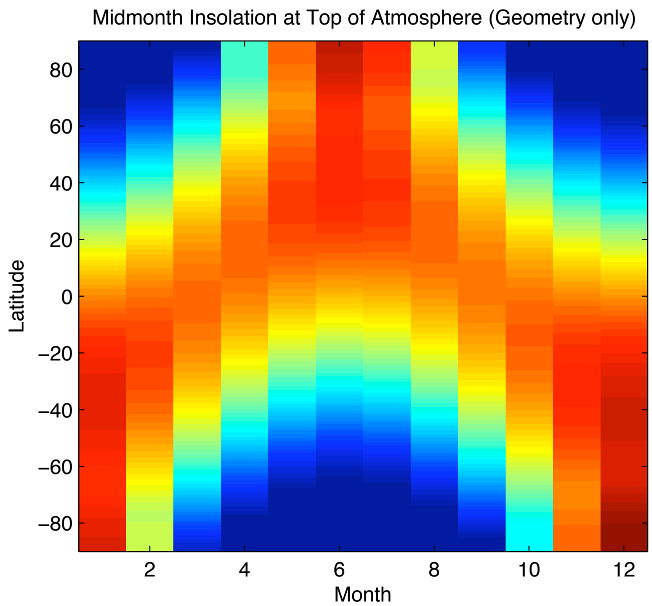

Figure 1: Average daily intensity of insolation at the top of the atmosphere at mid-month, calculated only using the geometric relations of orbit [Hartman, 1994, Spencer, 1971].

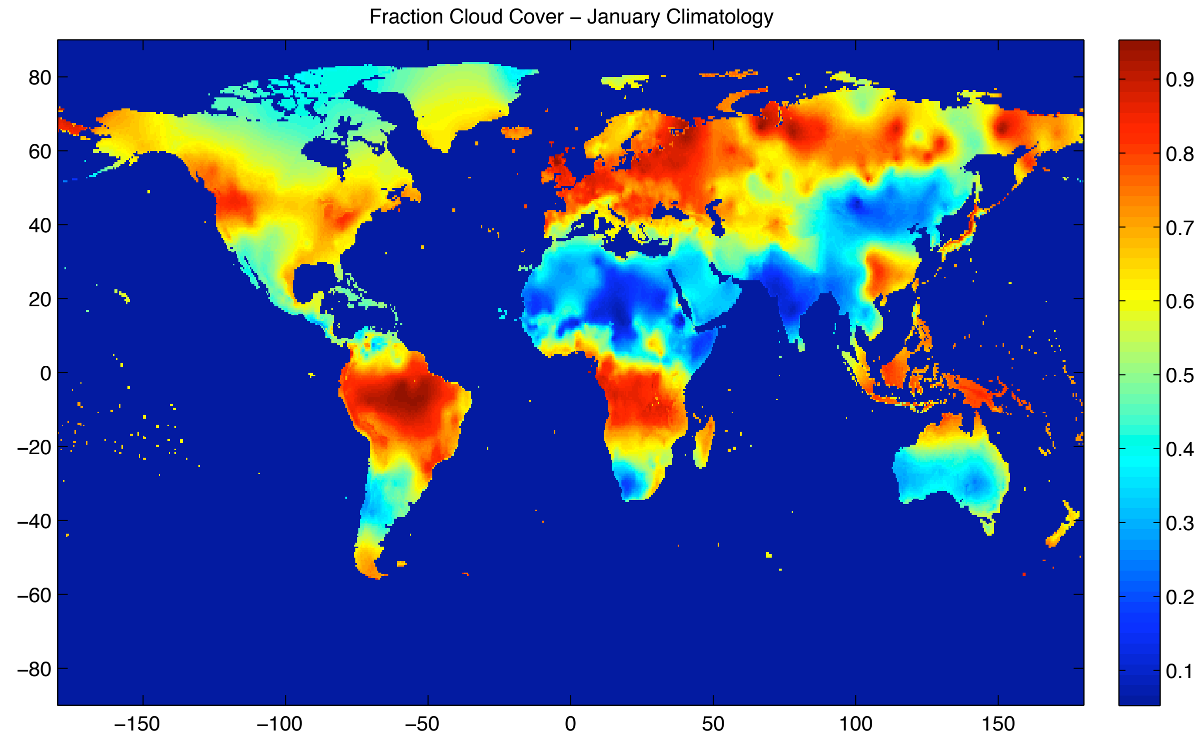

Figure 2: Example of monthly average cloud cover fraction climatology (observations) [Mitchell and Jones, 2005].

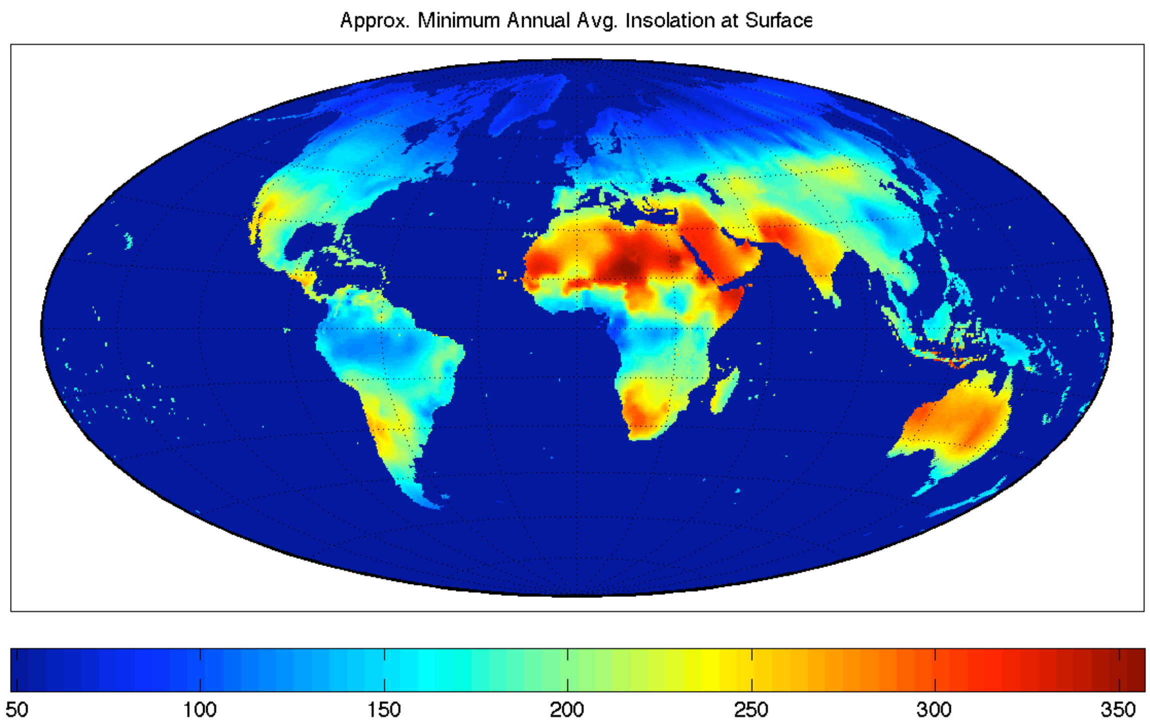

Figure 3: Combining insolation from geometry and cloud cover (assuming a constant, conservative albedo of 0.85 for all clouds) by month, then forming an annual average.

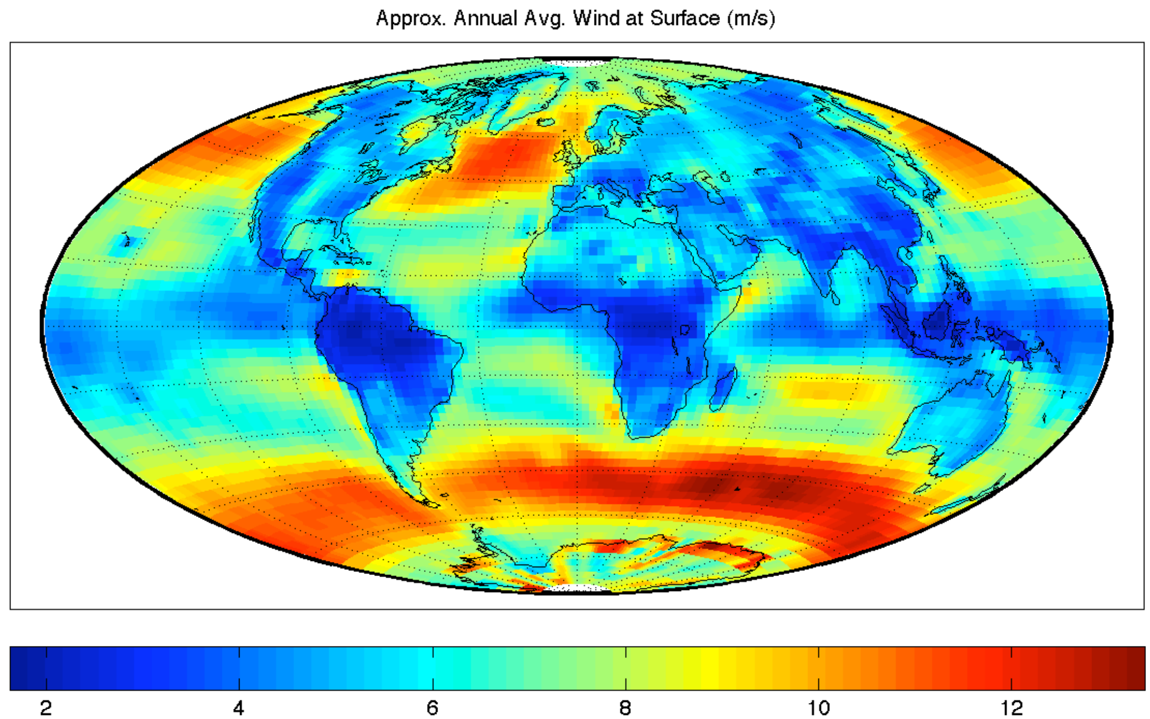

Figure 4: Annual average surface wind velocity (reanalysis) [Trenberth et al., 1989].

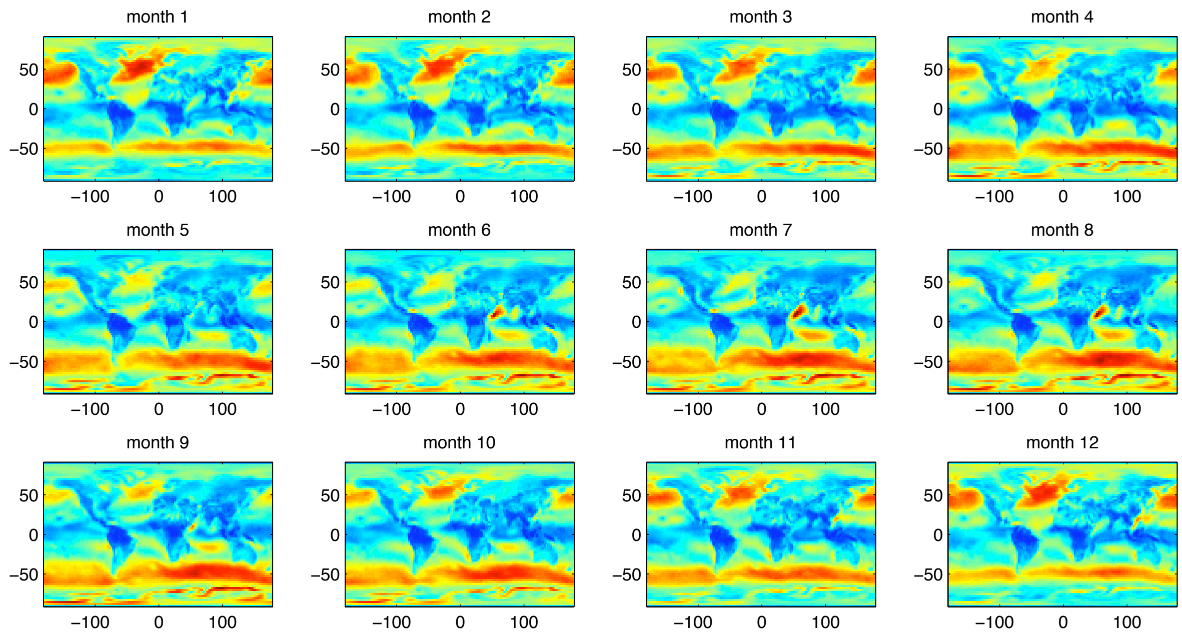

Figure 5: Monthly average surface wind velocity (reanalysis) [Trenberth et al., 1989].

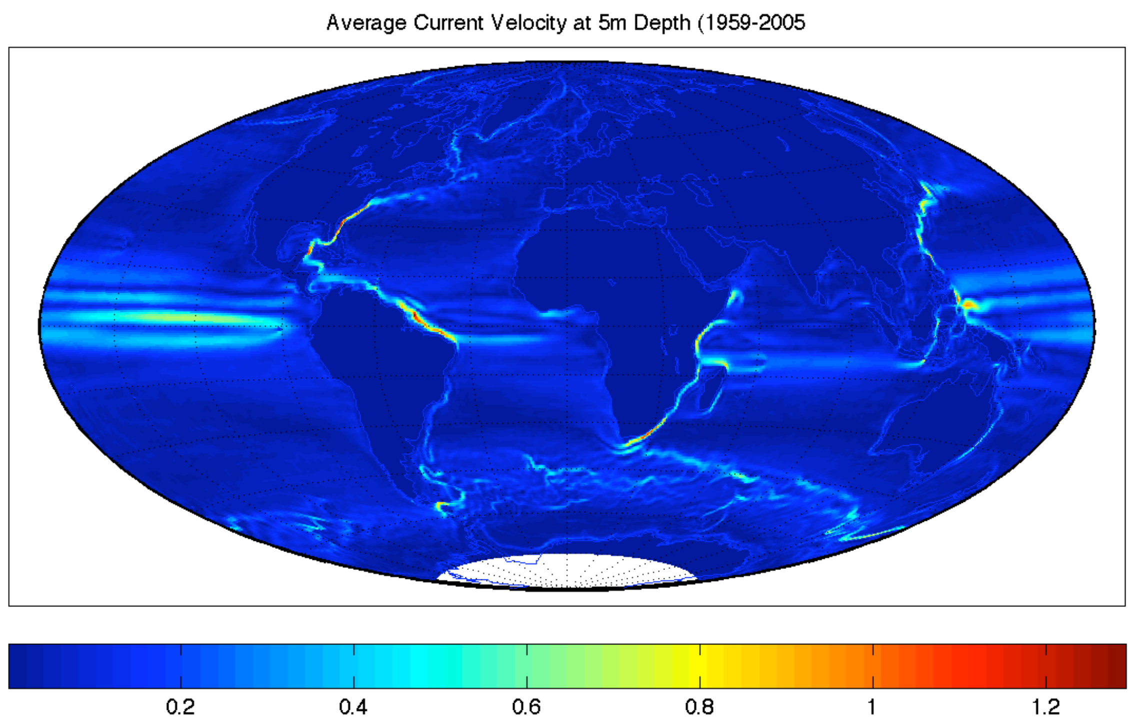

Figure 6: Average ocean current velocity at 5 meters depth (reanalysis) [Carton and Giese, 2007].

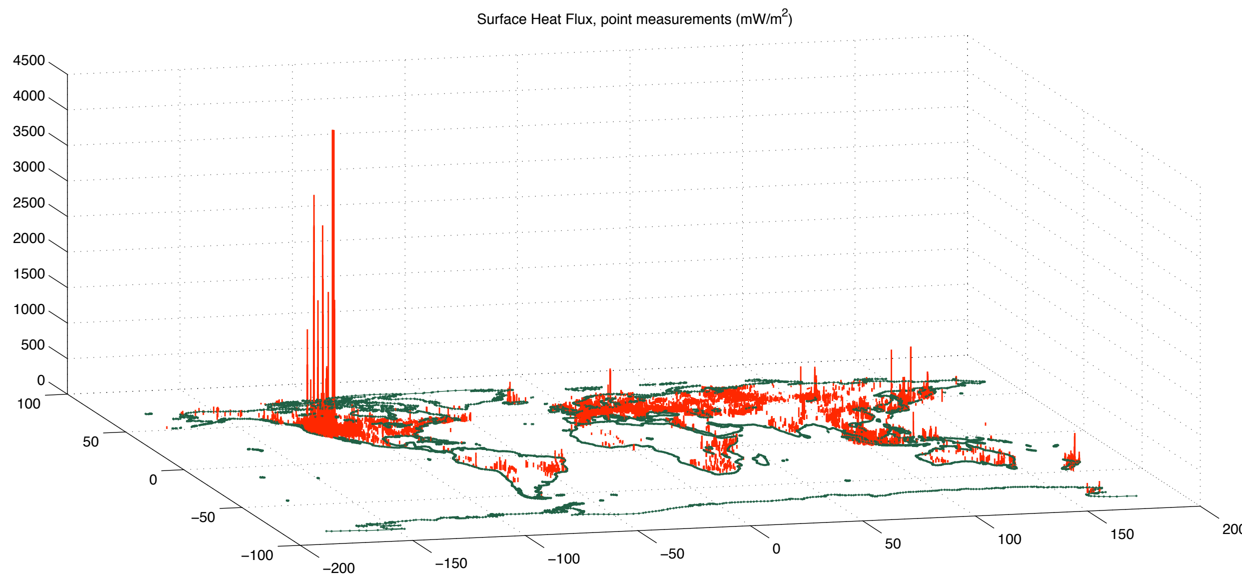

Figure 7: Continental observations of geothermal heat flux [International Heat Flow Commission, 2008].

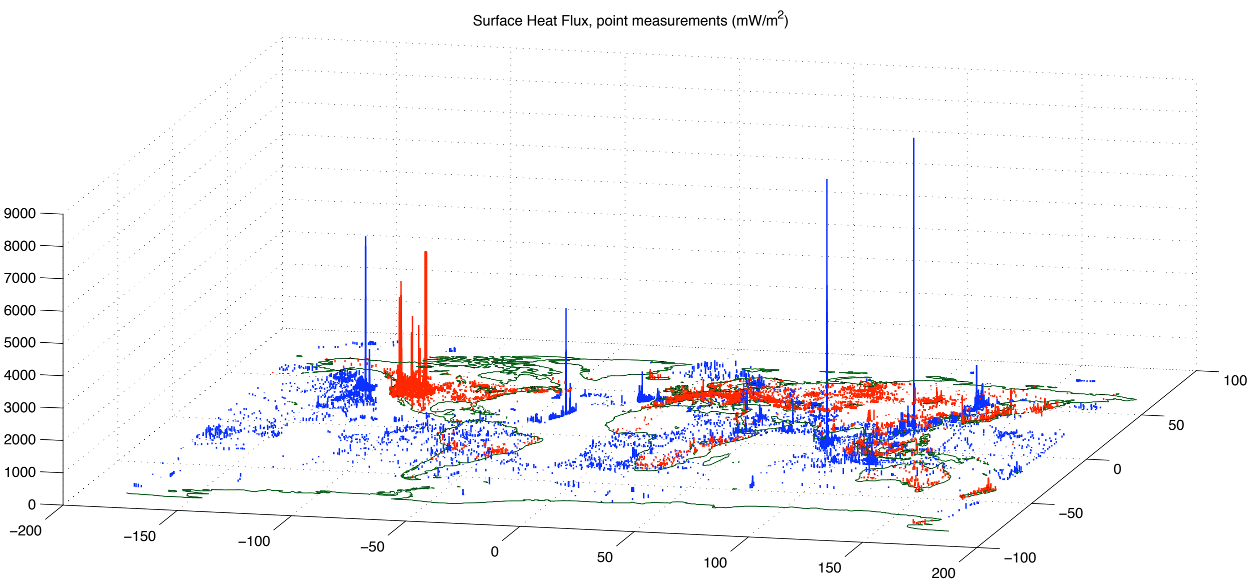

Figure 8: All observations of geothermal heat flux [International Heat Flow Commission, 2008]. Red are continental observations and blue are marine observations.